C. R. Geoscience 347 (2015) 358–367

Contents lists available at ScienceDirect

Comptes Rendus Geoscience

www.sciencedirect.com

Hydrology, Environment (Surface Geochemistry)

Mass-dependent and mass-independent fractionation of mercury isotopes in precipitation from Guiyang, SW China

Zhuhong Wang [a,b], Jiubin Chen [a,*], Xinbin Feng [a], Holger Hintelmann [c], Shengliu Yuan [a,b], Hongming Cai [a,b], Qiang Huang [a], Shuxiao Wang [d], Fengyang Wang [d]

[a] State Key Laboratory of Environmental Geochemistry, Institute of Geochemistry, Chinese Academy of Sciences, Guiyang 550002, China
[b] University of Chinese Academy of Sciences, Beijing 100039, China
[c] Chemistry Department, Trent University, Peterborough, ON K9J 7B8, Canada
[d] State Key Joint Laboratory of Environment Simulation and Pollution Control, School of Environment, Tsinghua University, Beijing 100084, China

ARTICLE INFO

Article history:
Received 30 November 2014
Accepted after revision 14 February 2015
Available online 29 April 2015

Keywords:
Mass-dependent fractionation
Mass-independent fractionation
Mercury isotopes
Chinese precipitation
Source tracing

ABSTRACT

The isotopic composition of mercury (Hg) is increasingly used to constrain the sources and pathways of this metal in the atmosphere. Though China has the highest Hg production, consumption and emission in the world, Hg isotope ratios are rarely reported for Chinese wet deposition. In this study, we examined, for the first time outside North America, both mass-dependent fractionation (MDF, expressed as δ^{202}Hg) and mass-independent fractionation of odd (odd-MIF, Δ^{199}Hg) and even (even-MIF, Δ^{200}Hg) Hg isotopes in 15 precipitation samples collected from September 2012 to August 2013 in Guiyang (SW China). All samples displayed significant negative δ^{202}Hg (−0.44 ∼ −4.27‰), positive Δ^{199}Hg (+0.19 to +1.16‰) and slightly positive Δ^{200}Hg (−0.01‰ to +0.20‰). Potential sources of Hg in precipitation were identified by coupling both MDF and MIF of Hg isotopes with a back-trajectory model. The results showed that local emission from coal-fired power plants and cement plants and western long-range transportation are two main contributing sources, while the contribution of Hg from south wind events would be very limited on an annual basis. The relatively lower Δ^{200}Hg values in Guiyang precipitation may indicate a dilution effect by local sources and/or insignificant even-MIF in the tropopause contribution of this subtropical region. Our study demonstrates the usefulness of isotope fractionation, especially MIF for tracing sources and pathways of Hg in the atmosphere.

1. Introduction

Mercury (Hg) is a hazardous metal with high toxicity and extreme mobility. The bioaccumulation and biomagnification of its toxic form mono-methylmercury (MMHg) in aquatic food webs may pose significant threats to human health and the environment (Sonke et al., 2013). The atmosphere plays a critical role in the global biogeochemical cycle of Hg and is an important reservoir of Hg; for example, more than 6×10^9 g of mercury were found in the single troposphere (Blum, 2011; Lin and Pehkonen, 1998; Slemr et al., 1985; Strok et al., 2015). Hg could be naturally released or re-emitted into the atmosphere by volcanic eruptions, forest fires, sea salt

* Corresponding author.
E-mail address: chenjiubin@vip.gyig.ac.cn (J. Chen).

http://dx.doi.org/10.1016/j.crte.2015.02.006
1631-0713/

spray, wind-blown soil particles, and biogenic aerosols. Mercury can also be emitted into the atmosphere by human activities, such as coal combustion, cement production, non-ferrous metal smelting and waste incineration (Streets et al., 2005; Wang et al., 2014b). Anthropogenic emission is about three times that resulting from natural processes (Blum et al., 2014; Mason et al., 1994) and could reach remote areas, such as Tibet and Arctic areas (Douglas et al., 2008; Huang et al., 2012). Hg mainly exists as gaseous elemental Hg (Hg^0), divalent reactive gaseous Hg (Hg(II)) and particle-bound Hg (Hg_p) in the atmosphere. Hg^0 is relatively inert and has a residence time of several months to one year, which allows for long-distance transport (Schroeder and Munthe, 1998). However, both Hg (II) and Hg_p are of high water solubility and thus deposit easily (Schroeder and Munthe, 1998). These atmospheric mercury species undergo complex physical and chemical processes, which make it challenging to identify the sources and pathways of Hg in the atmosphere and to evaluate its impact on surface ecosystems after deposition (Fu et al., 2010, 2012; Sonke, 2011; Wang et al., 2014b, 2006).

Mercury isotope signature is a useful tool for understanding Hg sources and the potential processes that Hg has undergone in the aqueous environment including precipitation and surface waters (Sonke and Blum, 2013). The advent of MC–ICP–MS has allowed for accurately measuring Hg isotopic composition, which sheds light on the global Hg cycle (Chen et al., 2012; Point et al., 2011; Sherman et al., 2011; Yin et al., 2014). Previous studies have reported both mass-dependent fractionation (MDF) and mass-independent fractionation (MIF) of Hg isotopes in nature. Laboratory experiments showed that MDF could occur in almost all kinetic and equilibrium reactions (Blum et al., 2014), while MIF of odd Hg isotopes (odd-MIF, Δ^{199}Hg) could only be triggered by special processes, such as photochemical reduction of Hg(II), photochemical degradation of MMHg, equilibrium evaporation, and abiotic dark reduction (Bergquist and Blum, 2007; Estrade et al., 2009; Zheng and Hintelmann, 2010b; Zheng et al., 2007). MDF has been proven to largely expand our understanding of the processes that constrain Hg distribution in various environments (Bergquist and Blum, 2009). The observation of odd-MIF greatly amplified the utilization of Hg isotopes because MIF could serve as the fingerprint of specific chemical pathways. Intriguingly, recent studies also reported MIF of even Hg isotopes (even-MIF, Δ^{200}Hg) in mainly atmospheric samples, highlighting the importance of investigating Hg isotopes in atmospheric deposition, by which Hg enters into terrestrial ecosystems (Chen et al., 2012; Gratz et al., 2010; Sherman et al., 2010, 2011). However, due to the very low concentration (ng/L level), Hg isotopes in precipitation are rarely reported (Chen et al., 2012; Gratz et al., 2010; Sherman et al., 2010, 2011).

China is the largest coal producer and consumer in the world, and is considered as the largest global atmospheric Hg contributor (Fu et al., 2010; Wang et al., 2014b; Yin et al., 2014). However, Hg isotopic characteristic in precipitation from China remains unknown. Guiyang is the capital city of the province of Guizhou (SW China), and possesses a large amount of coal and mercury mines, and is considered as an important Hg emission area in China (Feng and Qiu, 2008). Investigation of Hg isotopic signatures in this region could thus provide useful information on national Hg emission and deposition budgets in China. In this study, we determined the isotopic composition of Hg in precipitation from Guiyang collected from September 2012 to August 2013. This is the first study on Hg isotopic ratios in Chinese precipitation. The objectives of this study are:

- to characterize mercury isotopic signatures in precipitation in China;
- to identify the possible sources of Hg in Guiyang precipitation;
- to verify whether the observation of odd-MIF and even-MIF in North America precipitation results from a global phenomenon.

2. Materials and methods

2.1. Materials and reagents

All reagents (BrCl, HNO_3, HCl, L-cysteine, $NH_2OH{\cdot}HCl$, $SnCl_2$) used in this study were analytical grade and prepared in the clean room. The water was 18.2 MΩ/cm ultrapurified Milli-Q water (Millipore). The vessels were of glass or Teflon, and were consecutively washed with 2% BrCl (for two days), 20% HNO_3 (for one day) and Milli-Q water. Then, all the high borosilicate glass vessels were heated in a muffle furnace at 500 °C for an hour to remove trace Hg before their use. All the samples were collected using "U"-type Teflon board (surface area ~ 1.5 m^2 each) connected with a large glass beaker (volume of 5 L each). Before sampling, the samplers were cleaned using 10% HNO_3 then with Milli-Q water. The blank of the whole collecting system was accessed by processing 1 L of Milli-Q water and was about 15 pg ($n = 4$). The anion-exchange resin AG1-X4 (200–400 mesh, Bio-rad®) was used for pre-concentrating Hg from precipitation samples (Chen et al., 2010). NIST SRM 3133 Hg and two other Hg standards (Fluka and UM-Almadén, provided by J. Wiederhold and J. Blum) solutions were used as reference materials (also see Bergquist and Blum, 2007; Blum and Bergquist, 2007; Chen et al., 2010, 2012; Jiskra et al., 2012).

2.2. Field settings and sampling

The sampling site is shown in Fig. 1. Fifteen precipitation samples were collected on a building roof at the Institute of Geochemistry, Chinese Academy of Sciences (IGCAS, 26.35°N, 106.73°E), Guiyang, Guizhou, China, from September 2012 to August 2013. Guiyang is located in a subtropical region of the Yunnan–Guizhou Plateau. In general, our sampling site was constrained by two primary wind directions: west, southeast, with west wind dominated for most of the sampling period (from 9/2012 to 5/2013). Owing to low Hg concentration in precipitation (Table 1), a large volume of samples was needed to obtain

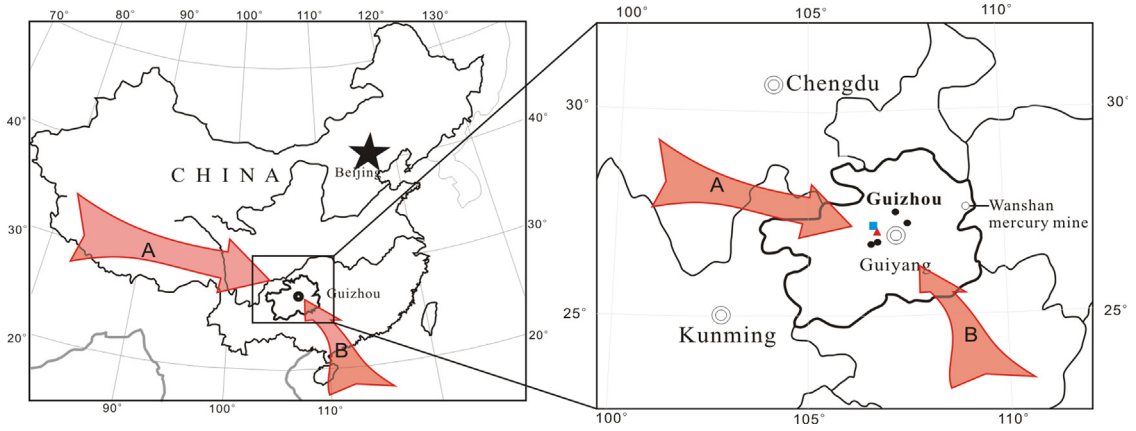

Fig. 1. (Color online.) Map of sampling site. All precipitation samples were collected at Guiyang City, Guizhou, China. The arrows indicate the main wind directions, with the west wind (A) dominated for most period of the year, while southeast wind (B) only existed in the short term (June to August). The red triangle, black dots, and the blue square represent the coal-fired power plants (CFPPs), cement plants and the aluminum smelter, respectively.

sufficient Hg (40 ng) (Chen et al., 2010) for accurate Hg isotopic composition determination. All samples were collected from the beginning to the end of a single precipitation event. Following collection, the samples were filtered soon using a pre-cleaned high borosilicate glass cone-shaped filtration device with a 0.45-μm mixed cellulose membrane filter. The blank of the filtration system was 9 pg ($n = 7$). The first 200 mL of filtered samples were abandoned.

2.3. Hg pre-concentration

After filtration, samples were digested with 0.5% 2 M BrCl for about 12 h to eliminate the organic matter, then 0.05% $NH_2OH{\cdot}HCl$ was added to neutralize the excess BrCl. Afterwards, the samples were acidified with 6 M to 0.1 M HCl and stored at 4 °C. All these samples were pre-concentrated using the protocol developed by Chen et al. (2010) as soon as possible. The borosilicate glass column charged with 0.5 mL AG 1 × 4 resin was first cleaned with 10 mL of 0.05% L-cysteine in 4 M HNO_3, 10 mL of 2 M HNO_3, and 10 mL of ultrapurified Milli-Q water, then conditioned with 10 mL of 0.1 M HCl. The pre-treated precipitation samples were loaded onto the column at a flow rate of about 3.5 mL/min controlled by a peristaltic pump. When loading was finished, the column was rinsed with 10 mL of 0.1 M HCl to remove the matrix. Finally, Hg was eluted in 10 mL of 0.5 M HNO_3 with 0.05% L-cysteine. The average process blank is about 70 pg, which is ignorable compared to Hg (up to 40 ng) needed for the Hg isotope composition determination. One more step, i.e. rinsing the column with 10 mL of 0.05% L-cysteine in 4 M HNO_3 was conducted to make sure that all loaded Hg was collected in the elution. The Hg pre-concentration solution was digested with BrCl again for at least 12 h to digest the excess L-cysteine and 20% $NH_2OH{\cdot}HCl$ (1/10 volume of BrCl) was added before the Hg isotope ratio determination (Chen et al., 2010, 2012).

Table 1
Hg concentrations and isotope values in 15 precipitation samples collected in Guiyang (SW China) and one snow sample from Nam co (Tibetan plateau, West China).

ID	Sample	Collection date	T (°C)	Event	Volume (L)	Hg (ng/L)	δ^{202}Hg (‰)	Δ^{199}Hg (‰)	Δ^{200}Hg (‰)	Δ^{201}Hg (‰)
R1 ($n = 1$)	Rain	21/09/12	15.5	S	3.05	3.75	−0.65 ± 0.10	0.19 ± 0.04	−0.01 ± 0.02	0.21 ± 0.04
R2 ($n = 1$)	Rain	26/12/12	2.75	S	3.2	6.62	−0.71 ± 0.10	1.05 ± 0.04	0.01 ± 0.02	0.90 ± 0.04
R3 ($n = 2$)	Rain and Snow	08/01/13	−0.25	S	6.07	16.18	−1.16 ± 0.04	1.16 ± 0.04	0.04 ± 0.02	0.96 ± 0.02
R4 ($n = 2$)	Snow	09/01/13	0	S	9.7	9.02	−0.62 ± 0.02	0.90 ± 0.04	0.00 ± 0.04	0.61 ± 0.00
R5 ($n = 2$)	Rain	19/03/13	15.5	S	6.23	10.21	−0.78 ± 0.08	0.73 ± 0.04	0.02 ± 0.06	0.62 ± 0.06
R6 ($n = 2$)	Rain	26/03/13	16.25	S	11.24	23.84	−0.92 ± 0.10	0.48 ± 0.00	0.09 ± 0.00	0.48 ± 0.02
R7 ($n = 2$)	Rain	01/04/13	13	S	6.56	6.54	−0.83 ± 0.04	0.40 ± 0.02	0.05 ± 0.02	0.35 ± 0.02
R8 ($n = 2$)	Rain	23/04/13	17.5	S	6.12	14.76	−0.66 ± 0.00	1.09 ± 0.04	0.14 ± 0.06	1.03 ± 0.08
R9 ($n = 1$)	Rain	07/05/13	19.5	S	6.5	3.73	−1.69 ± 0.10	0.39 ± 0.04	0.08 ± 0.02	0.37 ± 0.04
R10 ($n = 1$)	Rain	08/05/13	19	S	6.7	3.88	−0.44 ± 0.10	0.52 ± 0.04	0.10 ± 0.02	0.60 ± 0.04
R11 ($n = 1$)	Rain	25/05/13	21	S	5.1	4.03	−0.88 ± 0.10	0.45 ± 0.04	0.14 ± 0.02	0.35 ± 0.04
R12 ($n = 1$)	Rain	09/06/13	17.5	S	6.45	6.68	−1.21 ± 0.10	0.47 ± 0.04	0.20 ± 0.02	0.44 ± 0.04
R13 ($n = 1$)	Rain	04/07/13	24.5	S	9.3	11.75	−1.22 ± 0.10	0.75 ± 0.04	0.18 ± 0.02	0.82 ± 0.04
R14 ($n = 1$)	Rain	04/08/13	24.5	S	8.48	8.38	−4.27 ± 0.10	0.27 ± 0.04	0.03 ± 0.02	0.18 ± 0.04
R15 ($n = 1$)	Rain	24/08/13	22	S	8.67	3.60	−0.66 ± 0.10	0.46 ± 0.04	0.14 ± 0.02	0.44 ± 0.04
$R_{Nam\ co}$	Snow	22/10/13	−4	S	9.7	2.03	−0.1 ± 0.10	1.57 ± 0.04	0.12 ± 0.03	1.53 ± 0.02

n: number of measurements; error bars are described in detail in the text; S: single precipitation event.

2.4. Hg isotope analysis

Hg isotope ratio measurements were performed on Nu MC–ICP–MS (Nu Instruments) at IGCAS or Xiamen University following previous published methods (Bergquist and Blum, 2007; Foucher and Hintelmann, 2006; Lin et al., 2015). The instrumental mass bias was corrected by sample-standard bracketing (SSB). The MDF of Hg isotopes is represented by delta notation (δ^xHg in ‰) and defined as the following equation (Blum and Bergquist, 2007):

$$\delta^x\mathrm{Hg} = ((^x\mathrm{Hg}/^{198}\mathrm{Hg})_{\mathrm{sample}}/(^x\mathrm{Hg}/^{198}\mathrm{Hg})_{\mathrm{std}} - 1) \times 1000 \quad (1)$$

where x = 199, 200, 201, 202, "std" is NIST SRM 3133 Hg solution. MIFs of both odd and even Hg isotopes were defined by the deviation from the theoretically predicted MDF (Blum and Bergquist, 2007):

$$\Delta^{199}\mathrm{Hg} = \delta^{199}\mathrm{Hg} - 0.252 \times \delta^{202}\mathrm{Hg} \quad (2)$$

$$\Delta^{200}\mathrm{Hg} = \delta^{200}\mathrm{Hg} - 0.502 \times \delta^{202}\mathrm{Hg} \quad (3)$$

$$\Delta^{201}\mathrm{Hg} = \delta^{201}\mathrm{Hg} - 0.752 \times \delta^{202}\mathrm{Hg} \quad (4)$$

The repeated measurements of UM-Almadén and Fluka standards gave the long-term average δ^{202}Hg values of –0.49 ± 0.10‰ (n = 45, 2σ) and –1.39 ± 0.10‰ (n = 10, 2σ), respectively, in accordance with previous studies (Bergquist and Blum, 2007; Blum and Bergquist, 2007; Chen et al., 2010, 2012; Jiskra et al., 2012). The uncertainty was calculated as the 2σ external standard deviations of repeated analyses for both standards and samples with multiple measurements (e.g., R3 to R8). The obtained 2σ uncertainties from long-term measurements of UM-Almadén Hg standard were respectively 0.10‰, 0.04‰, 0.02‰, 0.04‰ for δ^{202}Hg, Δ^{199}Hg, Δ^{200}Hg, Δ^{201}Hg and were applied to samples measured only once due to the limited sample volume (Table 1).

3. Results and discussion

3.1. Mercury concentration (THg) and annual Hg isotopic variation

THg of all Guiyang precipitation samples varied from 3.6 ng/L to 23.8 ng/L, with an average value of 9 ng/L (Table 1). These values are relatively higher than those in precipitation from Mt. Leigong (about 4 ng/L, Fu et al., 2010), which were considered as a background area in Guizhou Province; they are similar to the rain in Peterborough and Great Lakes region (5.44 and 14.3 ng/L, respectively) (Chen et al., 2012; Gratz et al., 2010), but lower than that (~ 51.8 ng/L) of precipitation near a coal-fired plant in Florida (USA) (Sherman et al., 2011).

All precipitation samples displayed significant negative δ^{202}Hg and positive Δ^{199}Hg (Fig. 2). δ^{202}Hg values varied from –0.44‰ to –4.27‰, with the average –1.11‰, and the Δ^{199}Hg variation was from +0.19‰ to +1.16‰, with the average +0.62‰. Slightly positive Δ^{200}Hg was also determined in about half of the samples, with Δ^{200}Hg varied between –0.01 and +0.20‰, averaging +0.08‰.

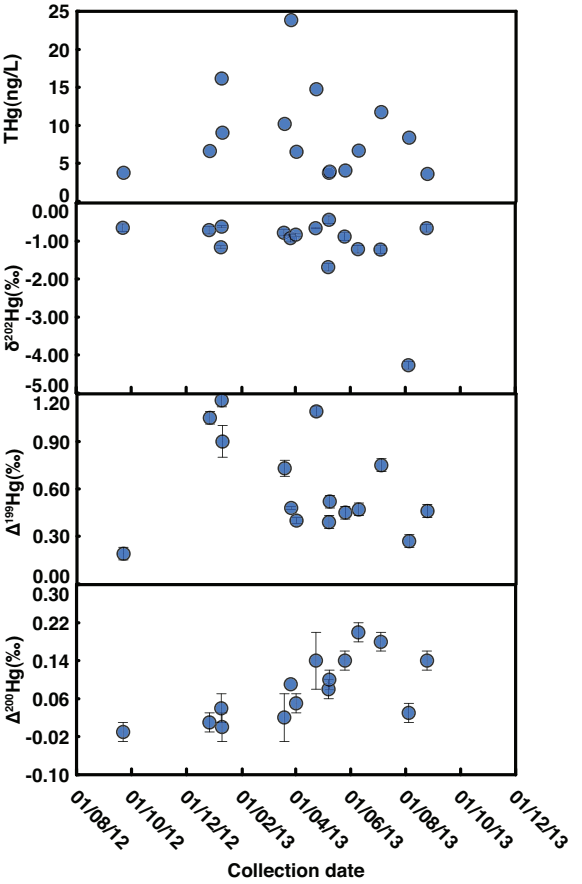

Fig. 2. (Color online.) Annual variation of Hg concentration (a), δ^{202}Hg (b), Δ^{199}Hg (c) and Δ^{200}Hg (d) in precipitation from Guiyang, Guizhou, China. Error bars are 2σ external standard deviations for samples with multiple measurements, or ± 0.10‰, ± 0.04‰ and ± 0.02‰ for δ^{202}Hg, Δ^{199}Hg and Δ^{200}Hg for samples measured only once, respectively.

3.2. Contribution of local sources to Hg in precipitation

Hg released from coal-fired power plants (CFPPs) and cement plants could be the main local sources for Hg in Guiyang precipitation. Previous studies have reported that the main anthropogenic mercury emissions in China are derived from CFPPs, cement plants, non-ferrous metal smelters and other industries (Streets et al., 2005; Wang et al., 2014b). Among those, coal combustion was the leading mercury source (Zhang et al., 2012a), and contributed, for example, about 2053 T to the total Hg emission in China between 1995 and 2003 (Wu et al., 2006). Recently, electrostatic precipitators (ESPs) and wet flue gas desulfurizations (WFGDs) were widely installed to reduce Hg emission due to power plants. ESPs can remove nearly all the Hg_p, and WFGDs could also get rid of a large proportion of Hg(II) (67–98%) (Zhang et al., 2013a, b). Therefore, Hg^0 and Hg(II) are likely the main forms of mercury released into the atmosphere by power plants. Though these efforts have considerably lessened CFPPs Hg emission, atmospheric pollution by Hg emitted by CFPPs is still an important issue due to the wide distribution of

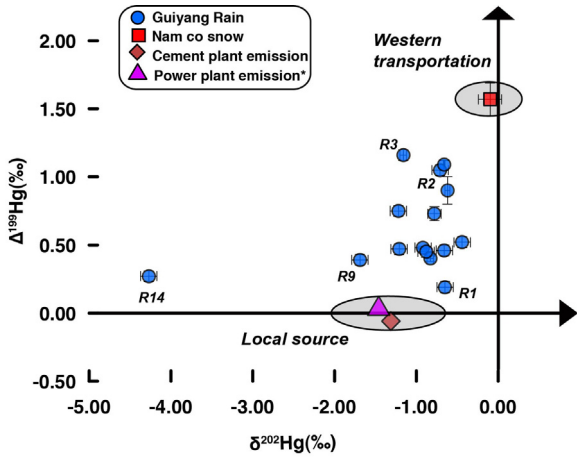

Fig. 3. (Color online.) Hg isotopic compositions (odd-MIF and δ^{202}Hg) of precipitation samples (blue points) in Guiyang and Nam co snow (red square) on the Tibetan Plateau. The calculated isotope ratios of Hg emitted from local coal-fired power plants (pink triangle) and from a cement plant (orange diamond) were also given for comparison. Error bars are 2σ external standard deviations for samples with multiple measurements, or ±0.10‰ and ±0.04‰ for δ^{202}Hg and Δ^{199}Hg for samples measured only once, respectively. *Isotope ratios were calculated based on the data reported in Sun et al. (2013, 2014) and Yin et al. (2014).

numerous plants. The province of Guizhou and its surrounded area are one of the major coal producing regions in China (produced about 200 million tons in 2014), where the coal is characterized by high Hg content (Feng and Qiu, 2008). Interestingly, about 80% of coal produced in this region was locally consumed. There are totally 18 CFPPs in the province of Guizhou, with the largest Tangzhai plant located at Qingzhen City, just outside Guiyang. Therefore, local Hg emission from CFPPs may be an important contributing source of Hg in Guiyang precipitation (Fu et al., 2011).

As shown in Fig. 3, all precipitation samples were characterized by negative δ^{202}Hg values, with an average value of –1.11‰. Though previous studies have reported an average δ^{202}Hg of ~ –1.36‰ for local Guizhou coals (Sun et al., 2013, 2014; Yin et al., 2014), no Hg isotope data is available for local CFPPs emission up to now. Based on the fractionation factors (of about –0.50‰ for Hg_p and around zero for Hg(II)) and the Hg species ratios (Hg^0:Hg(II):Hg_p = 0.5:0.4:0.1) reported in Sun et al. (2014) for stack emission from typical CFPPs, we can estimate a mean δ^{202}Hg of about –1.46‰ for Hg (Hg(II) and Hg_p) emitted from local CFPPs, very close to the average value (–1.11‰) in precipitation. Coal burning from individual house in rural region may also contribute to Hg in the precipitation. Unfortunately, the Hg isotopic ratio of this emission was not measured. We suggest that Hg from these coals may undergo similar isotope fractionation process during simple combustion as reported in Sun et al. (2013), and thus exhibited δ^{202}Hg values close to those of CFPPs emission.

Except for the power plants, cement plants could also be a local Hg contributor in precipitation. It is worth mentioning that more than 90% of mercury in coal and raw materials of cement plants is emitted into the atmosphere, with Hg(II) as the major species, which accounts for 61–91% of the total mercury emission (Wang et al., 2014a). Recent studies reported a significant increase (up to three times relative to that in 1999) in Hg emission from cement plants in China (Streets et al., 2005; Wang et al., 2014a; Zhang et al., 2012b). There are four large cement plants (Hailuopanjiang, Qingzhenxinfa, Kaiyangzijiang, and Qingzhenxinan cement plants) in the Guiyang region. Hg(II) and Hg_p emitted from these local plants could be easily scavenged into precipitation, showing significant impact on local Hg deposition. At this stage, we are unaware of any available Hg isotope data for cement plant emission. We measured, in this study, Hg isotope ratios for both input and output solid samples (coal, clay, sandstone, limestone, steel slag, and cement clinker) collected at different procedural stages from a cement plant in adjacent Sichuan province, using the protocol developed by Huang et al. (2015). Based on these data, the weighted average Hg isotopic ratio of all input materials was calculated (see Appendix A and Table 2) and was about –1.32‰ for δ^{202}Hg. A further mass balance calculation using the model of Wang et al. (2014a) gave a δ^{202}Hg value of about –1.33‰

Table 2
Hg mass balance calculation and the Hg isotopic ratios in flue gas emitted from a cement plant in the adjacent Sichuan Province.

Sample	THg (ng/g)	Mass (t/d)	Percentage (%)	δ^{202}Hg (‰)	Δ^{199}Hg (‰)	Δ^{201}Hg (‰)
Input						
Coal	37.7	256.8	6.9[a]	–1.55 ± 0.10	–0.07 ± 0.04	–0.13 ± 0.04
Clay	17.2	962.7	11.8[a]	–1.79 ± 0.10	–0.22 ± 0.04	–0.29 ± 0.04
Sandstone	13.0	464.1	4.3[a]	–1.02 ± 0.10	0.04 ± 0.04	–0.03 ± 0.04
Limestone	12.8	4681.0	42.7[a]	–1.43 ± 0.10	–0.07 ± 0.04	–0.03 ± 0.04
Steel slag	111.5	431.7	34.3[a]	–1.02 ± 0.10	0.00 ± 0.04	0.03 ± 0.04
Total		6796.3	100[a]			
Output						
Cement clinker	0.9	3586.0	2.3[a]	–1.18 ± 0.10	0.00 ± 0.04	0.00 ± 0.04
Flue gas		3210.3	97.7[a]	–1.33[b]	–0.06[b]	–0.05[b]

[a] Percentage (mass balance) and Hg isotopic ratios in flue gas were calculated based on THg (concentration), Hg mass and Hg isotopic ratios of each input sample. The 2σ uncertainties (respectively ± 0.10‰, ± 0.04‰, ± 0.04‰ for δ^{202}Hg, Δ^{199}Hg and Δ^{201}Hg) obtained from long-term measurements (n = 45) of UM-Almadén Hg standard were applied to solid samples.
[b] Calculated Hg isotopic compositions for flue gas (see Appendix A).

for emitted flue gas (Appendix A), similar to the integrated value of input samples. Therefore, unlike the CFPPs, the processes in cement plants would not induce significant fractionation of Hg isotopes. Accordingly, this value was also close to the average δ^{202}Hg (−1.11‰) for precipitation samples. This may suggest that local emission from both CFPPs and cement plants was an important source of Hg in precipitation samples. For example, the samples R1 and R9 may have been strongly impacted by this local Hg emission (Fig. 3).

Emission from local smelters may contribute to the Hg budget in precipitation as well. However, given the fact that Hg emission from non-ferrous metal smelters considerably decreased during the last decade in China (from about 147.6 t to 97.4 T) (Streets et al., 2005; Wang et al., 2013) and that the proportion of Hg emitted from limited number of smelters in Guizhou Province was relatively low (about 0.3–13.5% of initial total Hg) (Zhang et al., 2012b), the contribution of local non-ferrous metal smelting would be insignificant to Hg in precipitation. For example, the largest aluminum smelting plant of Guizhou Province (at North Guiyang) evaded only about 171 kg of Hg in 2006 (Fu et al., 2011), which may indicate limited impact on wet Hg deposition. Meanwhile, we cannot exclude the contribution of other anthropogenic sources (e.g., vehicle exhausts, house cooking) to Hg in our precipitation samples.

The contribution of local sources was also confirmed by the NOAA-HYSPLIT Hg back-trajectory model. The air mass trajectories with heights of 500, 1000 and 3000 m above ground level (AGL) were monitored to trace the Hg pathways in the atmosphere. The model showed that, for instance for sample R1, its air masses of 500 and 1000 AGL came mainly from the adjacent area and stayed several days in the region (Fig. S1). Hg emitted from local CFPPs and cement plants may thus be incorporated in these air masses, being an important contributing source to Hg in precipitation.

3.3. Possible Hg isotope fractionation in the atmosphere

In this study, most precipitation samples have positive Δ^{199}Hg values (up to +1.16‰, Table 1), which cannot be explained by local emission from CFPPs and cement plants that did not show significant odd-MIF. Atmospheric biogeochemical processes may modify Hg isotopic signatures and induce odd-MIF after Hg emission from local sources (Sherman et al., 2011). Once emitted to the atmosphere, species Hg(II) can undergo various atmospheric processes. Though processes, such as adsorption, incorporation of Hg(II) into water droplets in the atmosphere could cause MDF (Wiederhold et al., 2010), they scarcely induce any odd-MIF. Given the very low concentration of MMHg, the only possible procedure inducing higher Δ^{199}Hg values in the atmosphere is the photoreduction of Hg(II) in water droplets (Chen et al., 2012; Gratz et al., 2010). The linear relationship between Δ^{199}Hg and Δ^{201}Hg can be used to identify specific process triggering odd-MIF. Experimental study showed that Hg(II) photoreduction can enrich heavier (e.g., ^{202}Hg) and odd (e.g., ^{199}Hg and ^{201}Hg) Hg isotopes in aqueous phase and induce a Δ^{199}Hg/Δ^{201}Hg slope of about 1.00

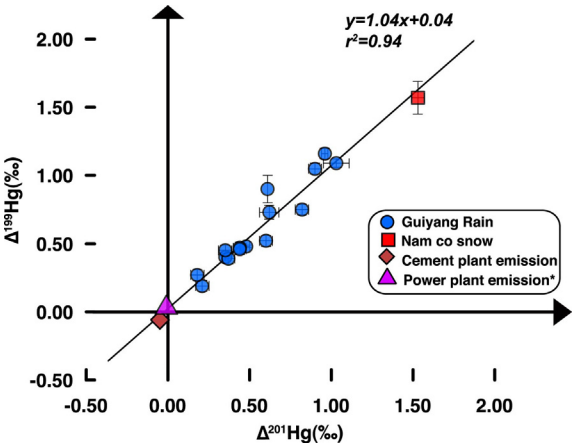

Fig. 4. (Color online.) Δ^{199}Hg vs. Δ^{201}Hg (‰) for precipitation samples in Guiyang (blue points) and one snow sample at Nam co (red square). The slope of 1.04 defined by all precipitation samples is in agreement with odd-MIF induced by photoreduction. *Isotope ratios were calculated based on the data reported in Sun et al. (2013, 2014) and Yin et al. (2014).

(Bergquist and Blum, 2007). In this study, all precipitation samples define a Δ^{199}Hg/Δ^{201}Hg slope of about 1.04 (Fig. 4), which is consistent with the result of previous photoreduction experiments and precipitation sample studies (Bergquist and Blum, 2007; Chen et al., 2012; Gratz et al., 2010; Sherman et al., 2010, 2011). This suggests that odd-MIF in Guiyang precipitation was possibly triggered by Hg(II) photoreduction, which may increase Δ^{199}Hg by about +0.04‰ for initial emitted Hg(II) up to +1.16‰ in the final precipitation. However, Guiyang precipitation did not show a clear increase in δ^{202}Hg with Δ^{199}Hg (Fig. 3). This is in conflict with the results of photoreduction experiments (inducing significant higher MDF and odd-MIF in aqueous phase). Moreover, a simple Rayleigh model calculation based on the model given by Zheng and Hintelmann (2010a) showed that, in order to produce a Δ^{199}Hg of +1.16‰ for the residual Hg(II) in rainfall, about 42% of Hg(II) (with no odd-MIF and derived from local emission) from initial water solution should be photoreduced and released into the air. In this case, the calculated corresponding δ^{202}Hg in the ultimate atmospheric phase would be −0.26‰ for Hg emitted from CFPPs, and about −0.24‰ for Hg originated from cement plants. These values are relatively higher than the determined data (average δ^{202}Hg = −1.11‰). This suggests that, although in-cloud photoreduction could be a cause for the elevated Δ^{199}Hg, the effect of this process would not be dominant.

3.4. Contribution of long-range transport Hg

An alternative explanation for the high Δ^{199}Hg values in most samples is the contribution of other sources beside local emission, mainly derived from long-range transport Hg. Guiyang is dominantly influenced by western wind for most of the year. When wind from the west dominates, the Hg budget in precipitation in Guiyang may be strongly influenced by Hg derived from the west (e.g., Tibet plateau)

and transported by eastward wind. In order to access Hg isotopic composition in west Tibetan precipitation, a fresh snow sample collected on 22 October 2013 at Nam co (30.78°N, 90.99°E; altitude 4730 m) on the Tibetan plateau was analyzed. As shown in Table 1, this snow sample displayed negative δ^{202}Hg values (−0.10‰) and significant positive Δ^{199}Hg ones (+1.57‰). Given the fact that the residence time of Hg(II) in the atmosphere is on the order of days to weeks and Hg(II) is readily incorporated into droplets and adsorbed onto particles, Hg(II) derived from the Tibet plateau may be transported eastward and have an important impact on wet deposition in Guiyang. Interestingly, the isotopic data of Nam co snow was very close to values measured in samples with west-dominated wind (e.g., R2 and R3, Fig. 3), especially for Δ^{199}Hg. This similarity of odd-MIF may suggest a contribution of Hg(II) originated from the west (Tibet) to Hg in some precipitation samples in Guiyang after a moderate transport distance. This part of Hg may subsequently mix with local Hg emission and both would be incorporated into Guiyang precipitation. Thus, Hg in the precipitation samples would be a mixture of variable proportions of Hg derived from these two main sources (Figs. 3 and 4). In this case, samples R2 and R3 were more strongly impacted by west long-term transported Hg, while local contributions may dominate for R1 and R9. The western (Tibet) atmospheric Hg as an important contributor was further supported by the NOAA-HYSPLIT model. The calculation of the model showed that air masses associated with precipitation samples characterized by higher Δ^{199}Hg came mainly or passed through the Tibetan region, while those for samples with moderate Δ^{199}Hg clearly displayed combined impacts from both local and western sources. For example, the high elevation (1000 m and 3000 m AGL) air masses of sample R5 (Δ^{199}Hg = +0.73‰) showed mainly western origin, while its 500-m AGL air mass was more strongly influenced by local source (Fig. S2).

Compared to the case of the adjacent Guiyang region, point sources of Hg in the background area of the Tibetan plateau are less significant. According to previous studies, India was likely a significant atmospheric Hg pollution contributor to Tibet, especially during Indian monsoon season. Fu et al. (2012) suggested that the emission from northern India could be a significant source of atmospheric Hg at Waliguan (the northeastern Tibetan Plateau) during the sampling campaign from September 2007 to October 2008. Huang et al. (2012) also reported that 83% of Hg budget in Tibet was brought from India through atmospheric transport during the monsoon season. Other studies also showed that DDTs and PCBs of Tibet were strongly influenced by the Indian monsoon, with higher values in the monsoon season (May to September) and lower in the non-monsoon season (November to March) (Sheng et al., 2013). In this study, NOAA-HYSPLIT model (Fig. S3) indicated that the air masses associated with the Nam co snow sample at least partially came from northern India, showing the impact on Hg in Tibetan wet deposition. Though more work is needed to identify the exact sources of Hg in Tibet plateau, Tibetan atmospheric Hg may be largely transported in west wind events to the Guiyang region and present an important contribution to Hg in final precipitation samples.

We mention that sample R14 (Table 1) had very low δ^{202}Hg and Δ^{199}Hg values of −4.27‰ and of +0.27‰, respectively. This sample was collected during Southeast Asian monsoon (August 2013, Table 1). Trajectory analysis showed that air masses of this sample mainly came from the South China Sea and/or Indian Ocean (Fig. S4). The possible explanation for the very low δ^{202}Hg in R14 is thus the contribution of oceanic emission, which may be characterized by significantly negative δ^{202}Hg values, as reported (e.g., down to −3.88‰) by Rolison et al. (2013) for Hg^0 in the Grand Bay coastal area. Given

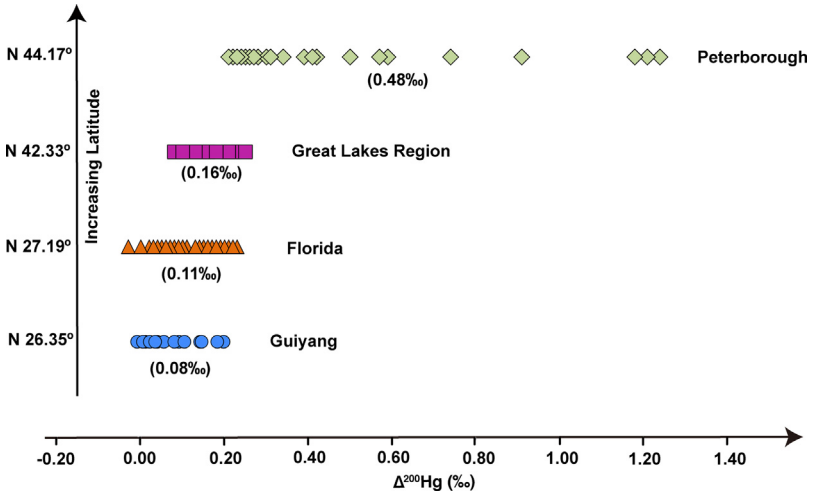

Fig. 5. (Color online.) MIF of even Hg isotopes in worldwide precipitation samples. The precipitation in Guiyang had relatively low Δ^{200}Hg values compared to the precipitation in North America. Taken as a whole, all samples displayed an increase in Δ^{200}Hg with latitude. Isotope data of precipitation from Peterborough, Great Lakes region and Florida are from Chen et al. (2012), Gratz et al. (2010), and Sherman et al. (2011), respectively. Data between brackets are the average Δ^{200}Hg values for each sampling site.

the fact that Southeast Asian monsoon dominated only a very short period of the year, the contribution of Hg from south wind events would be very limited on an annual basis.

3.5. Even-isotope MIF

In this study, about half of precipitation samples showed slightly positive Δ^{200}Hg, with relatively higher values in summer than in winter (Fig. 2 and Table 1). Slightly positive Δ^{200}Hg values were also determined in precipitation in Florida (USA) at low latitude (Sherman et al., 2011). Interestingly, relatively higher Δ^{200}Hg values were reported for Hg in precipitation at middle latitude (Chen et al., 2012; Gratz et al., 2010). As a whole, even-MIF of precipitation displayed thus an increase with latitude (Fig. 5). Though even-MIF was also observed with a compact fluorescent lamp (Mead et al., 2013), the potential mechanism inducing Δ^{200}Hg is still unclear. Chen et al. (2012) suggested that ^{200}Hg anomalies are likely related to photo-initiated Hg^0 oxidation at the tropopause. The lower Δ^{200}Hg in Guiyang precipitation and the decrease of even-MIF towards low-latitude regions would suggest that the subsequent stratosphere (to troposphere) incursion was characterized by relative lower Δ^{200}Hg in this subtropical region, or more likely, the even-MIF was largely diluted by the dominant local Hg contribution that had no ^{200}Hg anomaly.

4. Conclusions and implications

In this study, we reported for the first time Hg isotopic composition in precipitation from Guiyang, SW China, a country with the highest Hg production, consumption and emission in the world. All samples displayed negative MDF, significant positive odd-MIF and slightly positive even-MIF. These values are similar to those reported in most precipitation samples from North America (Chen et al., 2012; Gratz et al., 2010; Sherman et al., 2011), evidencing a general characteristic of Hg isotopic composition in atmospheric precipitation worldwide. Hg isotopic ratios were measured, for the first time, for solid samples collected from a local cement plant, and isotopic compositions of Hg emitted from this plant and also from local coal-fired power plants (CFPPs) were calculated. Our results demonstrated that the Hg budget in precipitation samples was mainly controlled by local emission from CFPPs and cement plants and western long-range transportation from the Tibetan plateau, and the effect of in-air processes would not be dominated. Though more work is needed to well explain the high Δ^{199}Hg in Tibetan precipitation, our study clearly illuminated the usefulness of odd-MIF for tracing Hg sources in the atmosphere. This work reported slightly positive Δ^{200}Hg (average +0.08‰) in the subtropical region, much lower than that found in mid latitude areas (Chen et al., 2012; Gratz et al., 2010). The increase of even-MIF with latitude supports again the conceptual model proposed by Chen et al. (2012). Further experimental study and theoretical work are needed to fully understand the mechanisms inducing even-MIF in the atmosphere. Our study indicated that Hg isotopes are a useful tool for tracing Hg pathways in regional and global biogeochemical cycle.

Acknowledgement

This work was funded by Natural Science Foundation of China (41273023, U1301231), the National "973" Program (2013CB430001), the Strategic Priority Research Program (No. XDB05030302) and the "hundred talent" project of the Chinese Academy of Sciences. The authors acknowledge reviewer J. Sonke and editor F. Chabaux, who greatly improved the quality of the manuscript. We thank Qixin Wu from Guizhou University for his constructive contribution.

Appendix A

To better identify the isotopic signature of Hg emitted from local cement plants and understand its relationship with Hg incorporated in Guiyang precipitation, we carried out a mass balance calculation to estimate Hg isotopic ratio in flue gas of a cement plant in the adjacent Sichuan Province, using the model of Wang et al. (2014a). Because no direct samples were collected from the stack emission, the data was calculated based on the weighted average Hg isotopic ratios of all input materials and solid products (cement clinker). Since gypsum is added and mixed with clinker under ambient temperature to form final cement, the Hg initially contained in gypsum is not released into flue gas and thus is not taken into account for mass balance calculation. We mention that the estimation was only conducted for one local cement plant, and much more work is needed to get an overall picture of Hg isotopic composition for local and national cement plant emission in China.

Firstly, the percentage of Hg in each input sample (i.e., coal, clay, sandstone, limestone and steel slag) relative to the total input could be estimated as follows:

$$P_i = \frac{T_i \times M_i}{\sum(T_i \times M_i)} \quad \text{(A1)}$$

where P_i, T_i and M_i represent for percentage, THg and the mass of each input sample, respectively (Table 1). Based on the mass balance ratio (P_i) and the measured Hg isotopic ratio of each input sample, the weighted average Hg isotopic ratio (δ^{202}Hg, Δ^{199}Hg) of the entire input could be calculated with the following formula:

$$\delta^{202}\mathrm{Hg}_{\mathrm{w-input}}(‰) = \sum (P_i \times \delta)^{202}\mathrm{Hg}_i \quad \text{(A2)}$$

$$\Delta^{xxx}\mathrm{Hg}_{\mathrm{w-input}}(‰) = \sum (P_i \times \Delta^{xxx}\mathrm{Hg}_i) \quad \text{(A3)}$$

where $\Delta^{xxx}Hg$ stands for Δ^{199}Hg or Δ^{201}Hg. By calculation, the weighted average δ^{202}Hg, Δ^{199}Hg and Δ^{201}Hg of the entire input are –1.32‰, –0.06‰ and –0.05‰, respectively.

Hg isotopic signatures in the stack flue gas could thus be estimated as follows:

$$\delta^{202}\mathrm{Hg}_{\mathrm{input}} = f_{\mathrm{clinker}}\delta^{202}\mathrm{Hg}_{\mathrm{clinker}} + (1 - f_{\mathrm{clinker}})\delta^{202}\mathrm{Hg}_{\mathrm{stack}} \quad \text{(A4)}$$

$$\Delta^{xxx}\mathrm{Hg}_{\mathrm{input}} = f_{\mathrm{clinker}}\Delta^{xxx}\mathrm{Hg}_{\mathrm{clinker}} + (1 - f_{\mathrm{clinker}})\Delta^{xxx}\mathrm{Hg}_{\mathrm{stack}} \quad \text{(A5)}$$

where *xxx* is 199 or 201, f_{clinker} is the fraction of Hg in the clinker. By calculation, δ^{202}Hg, Δ^{199}Hg and Δ^{201}Hg in emitted flue gas from the cement plant are –1.33‰, –0.06‰, and –0.05‰ (Table 2), respectively. These values are not significantly different from the initial weighted average Hg isotope ratios, since up to 98% Hg is emitted from the total input materials.

Appendix B. Supplementary data

Supplementary data associated with this article can be found, in the online version, at http://dx.doi.org/10.1016/j.crte.2015.02.006.

References

Bergquist, B.A., Blum, J.D., 2007. Mass-dependent and-independent fractionation of Hg isotopes by photoreduction in aquatic systems. Science 318, 417–420.

Bergquist, B.A., Blum, J.D., 2009. The odds and evens of mercury isotopes: applications of mass-dependent and mass-independent isotope fractionation. Elements 5, 353.

Blum, J.D., 2011. Applications of stable mercury isotopes to biogeochemistry. In: Baskaran, M. (Ed.), Handbook of Environmental Isotope Geochemistry. Springer, Berlin, Germany, pp. 229–245.

Blum, J.D., Bergquist, B.A., 2007. Reporting of variations in the natural isotopic composition of mercury. Anal. Bioanal. Chem. 388, 353–359.

Blum, J.D., Sherman, L.S., Johnson, M.W., 2014. Mercury isotopes in earth and environmental sciences. Annu. Rev. Earth Planet. Sci. 42, 249–269.

Chen, J., Hintelmann, H., Dimock, B., 2010. Chromatographic pre-concentration of Hg from dilute aqueous solutions for isotopic measurement by MC–ICP–MS. J. Anal. Atom. Spectrom. 25, 1402–1409.

Chen, J., Hintelmann, H., Feng, X., Dimock, B., 2012. Unusual fractionation of both odd and even mercury isotopes in precipitation from Peterborough, ON, Canada. Geochim. Cosmochim. Acta 90, 33–46.

Douglas, T.A., Sturm, M., Simpson, W.R., Blum, J.D., Alvarez-Aviles, L., Keeler, G.J., Perovich, D.K., Biswas, A., Johnson, K., 2008. Influence of snow and ice crystal formation and accumulation on mercury deposition to the Arctic. Environ. Sci. Technol. 42, 1542–1551.

Estrade, N., Carignan, J., Sonke, J.E., Donard, O.F.X., 2009. Mercury isotope fractionation during liquid-vapor evaporation experiments. Geochim. Cosmochim. Acta 73, 2693–2711.

Feng, X., Qiu, G., 2008. Mercury pollution in Guizhou, Southwestern China – an overview. Sci. Total Environ. 400, 227–237.

Foucher, D., Hintelmann, H., 2006. High-precision measurement of mercury isotope ratios in sediments using cold-vapor generation multi-collector inductively coupled plasma mass spectrometry. Anal. Bioanal. Chem. 384, 1470–1478.

Fu, X., Feng, X., Dong, Z., Yin, R., Wang, J., Yang, Z., Zhang, H., 2010. Atmospheric gaseous elemental mercury (GEM) concentrations and mercury depositions at a high-altitude mountain peak in South China. Atmos. Chem. Phys. 10, 2425–2437.

Fu, X., Feng, X., Liang, P., Zhang, H., Ji, J., Liu, P., 2012. Temporal trend and sources of speciated atmospheric mercury at Waliguan GAW station, northwestern China. Atmos. Chem. Phys. 12, 1951–1964.

Fu, X., Feng, X., Qiu, G., Shang, L., Zhang, H., 2011. Speciated atmospheric mercury and its potential source in Guiyang. China. Atmos. Environ. 45, 4205–4212.

Gratz, L.E., Keeler, G.J., Blum, J.D., Sherman, L.S., 2010. Isotopic composition and fractionation of mercury in Great Lakes precipitation and ambient air. Environ. Sci. Technol. 44, 7761–7770.

Huang, J., Kang, S., Zhang, Q., Yan, H., Guo, J., Jenkins, M.G., Zhang, G., Wang, K., 2012. Wet deposition of mercury at a remote site in the Tibetan Plateau: concentrations, speciation, and fluxes. Atmos. Environ. 62, 540–550.

Huang, Q., Liu, Y., Chen, J., Feng, X., Huang, W., Yuan, S., Cai, H., Fu, X., 2015. An improved dual-stage protocol to pre-concentrate mercury from airborne particles for precise isotopic measurement. J. Anal. Atom. Spectrom. 30, 957–966.

Jiskra, M., Wiederhold, J.G., Bourdon, B., Kretzschmar, R., 2012. Solution speciation controls mercury isotope fractionation of Hg(II) sorption to goethite. Environ. Sci. Technol. 46, 6654–6662.

Lin, C.J., Pehkonen, S.O., 1998. Oxidation of elemental mercury by aqueous chlorine (HOCl/OCl$^-$): implications for tropospheric mercury chemistry. J. Geophys. Res-Atmos. 103, 28093–28102.

Lin, H., Yuan, D., Lu, B., Huang, S., Sun, L., Zhang, F., Gao, Y., 2015. Isotopic composition analysis of dissolved mercury in seawater with purge and trap pre-concentration and a modified Hg introduction device for MC–ICP–MS. J. Anal. Atom. Spectrom., http://dx.doi.org/10.1039/c4ja00242c (in press).

Mason, R., Fitzgerald, W., Morel, F., 1994. The biogeochemical cycling of elemental mercury: anthropogenic influences. Geochim. Cosmochim. Acta 58, 3191–3198.

Mead, C., Lyons, J.R., Johnson, T.M., Anbar, A.D., 2013. Unique Hg stable isotope signatures of compact fluorescent lamp-sourced Hg. Environ. Sci. Technol. 47, 2542–2547.

Point, D., Sonke, J.E., Day, R.D., Roseneau, D.G., Hobson, K.A., Vander Pol, S.S., Moors, A.J., Pugh, R.S., Donard, O.F.X., Becker, P.R., 2011. Methylmercury photodegradation influenced by sea-ice cover in Arctic marine ecosystems. Nat. Geosci. 4, 188–194.

Rolison, J., Landing, W., Luke, W., Cohen, M., Salters, V., 2013. Isotopic composition of species-specific atmospheric Hg in a coastal environment. Chem. Geol. 336, 37–49.

Schroeder, W.H., Munthe, J., 1998. Atmospheric mercury – an overview. Atmos. Environ. 32, 809–822.

Sheng, J., Wang, X., Gong, P., Joswiak, D.R., Tian, L., Yao, T., Jones, K.C., 2013. Monsoon-driven transport of organochlorine pesticides and polychlorinated biphenyls to the Tibetan Plateau: three year atmospheric monitoring study. Environ. Sci. Technol. 47, 3199–3208.

Sherman, L.S., Blum, J.D., Johnson, K.P., Keeler, G.J., Barres, J.A., Douglas, T.A., 2010. Mass-independent fractionation of mercury isotopes in Arctic snow driven by sunlight. Nat. Geosci. 3, 173–177.

Sherman, L.S., Blum, J.D., Keeler, G.J., Demers, J.D., Dvonch, J.T., 2011. Investigation of local mercury deposition from a coal-fired power plant using mercury isotopes. Environ. Sci. Technol. 46, 382–390.

Slemr, F., Schuster, G., Seiler, W., 1985. Distribution, speciation, and budget of atmospheric mercury. J. Atmos. Chem. 3, 407–434.

Sonke, J.E., 2011. A global model of mass independent mercury stable isotope fractionation. Geochim. Cosmochim. Acta 75, 4577–4590.

Sonke, J.E., Blum, J.D., 2013. Advances in mercury stable isotope biogeochemistry. Chem. Geol. 336, 1–4.

Sonke, J.E., Heimbürger, L.E., Dommergue, A., 2013. Mercury biogeochemistry: paradigm shifts, outstanding issues and research needs. C R. Geoscience 345, 213–224.

Streets, D.G., Hao, J., Wu, Y., Jiang, J., Chan, M., Tian, H., Feng, X., 2005. Anthropogenic mercury emissions in China. Atmos. Environ. 39, 7789–7806.

Strok, M., Baya, A., Hintelmann, H., 2015. The mercury composition of Arctic coastal seawater. C. R. Geoscience 347, (this issue).

Sun, R., Heimbürger, L.E., Sonke, J.E., Liu, G., Amouroux, D., Berail, S., 2013. Mercury stable isotope fractionation in six utility boilers of two large coal-fired power plants. Chem. Geol. 336, 103–111.

Sun, R., Sonke, J., Heimbürger, L.-E., Belkin, H., Liu, G., Shome, D., Cukrowska, E., Liousse, C., Pokrovski, O., Streets, D.G., 2014. Mercury stable isotope signatures of world coal deposits and historical coal combustion emissions. Environ. Sci. Technol. 48, 7660–7668.

Wang, F., Wang, S., Zhang, L., Yang, H., Wu, Q., Hao, J., 2014a. Mercury enrichment and its effects on atmospheric emissions in cement plants of China. Atmos. Environ. 92, 421–428.

Wang, L., Wang, S., Zhang, L., Wang, Y., Zhang, Y., Nielsen, C., McElroy, M.B., Hao, J., 2014b. Source apportionment of atmospheric mercury pollution in China using the GEOS-Chem model. Environ. Pollut. 190, 166–175.

Wang, S., Zhang, L., Wu, Q., Wang, L., Wang, F., Hao, J., 2013. A new inventory on atmospheric mercury emissions from anthropogenic sources in China, 2000–2010. In: The 11th International Conference on Mercury as a Global Pollutant, Edinburgh Scotland, UK.

Wiederhold, J.G., Cramer, C.J., Daniel, K., Infante, I., Bourdon, B., Kretzschmar, R., 2010. Equilibrium mercury isotope fractionation between dissolved Hg(II) species and thiol-bound Hg. Environ. Sci. Technol. 44, 4191–4197.

Wu, Y., Wang, S., Streets, D.G., Hao, J., Chan, M., Jiang, J., 2006. Trends in anthropogenic mercury emissions in China from 1995 to 2003. Environ. Sci. Technol. 40, 5312–5318.

Yin, R., Feng, X., Chen, J., 2014. Mercury stable isotope compositions in coals from major coal producing fields in China and their geochemical and environmental implications. Environ. Sci. Technol. 48, 5565–5574.

Zhang, L., Daukoru, M., Torkamani, S., Wang, S., Hao, J., Biswas, P., 2013a. Measurements of mercury speciation and fine particle size distribution on combustion of China coal seams. Fuel 104, 732–738.

Zhang, L., Daukoru, M., Torkamani, S., Wang, S., Hao, J., Biswas, P., 2013b. Mercury speciation and fine particle size distribution on combustion of Chinese coals, Cleaner Combustion and Sustainable World. Springer, Berlin, Germany, 313–321.

Zhang, L., Wang, S., Meng, Y., Hao, J., 2012a. Influence of mercury and chlorine content of coal on mercury emissions from coal-fired power plants in China. Environ. Sci. Technol. 46, 6385–6392.

Zhang, L., Wang, S., Wu, Q., Meng, Y., Yang, H., Wang, F., Hao, J., 2012b. Were mercury emission factors for Chinese non-ferrous metal smelters overestimated? Evidence from onsite measurements in six smelters. Environ. Pollut. 171, 109–117.

Zheng, W., Foucher, D., Hintelmann, H., 2007. Mercury isotope fractionation during volatilization of Hg(0) from solution into the gas phase. J. Anal. Atom. Spectrom. 22, 1097–1104.

Zheng, W., Hintelmann, H., 2010a. Isotope fractionation of mercury during its photochemical reduction by low-molecular-weight organic compounds. J. Phys. Chem. A 114, 4246–4253.

Zheng, W., Hintelmann, H., 2010b. Nuclear field shift effect in isotope fractionation of mercury during abiotic reduction in the absence of light. J. Phys. Chem. A 114, 4238–4245.